Antioxidant Activity and Inhibition of ?-Glucosidase by Hydroxyl-functionalized 2-Arylbenzo[b]furans

ARTICLE *in* EUROPEAN JOURNAL OF MEDICINAL CHEMISTRY · FEBRUARY 2015

Impact Factor: 3.45 · DOI: 10.1016/j.ejmech.2015.02.024 · Source: PubMed

European Journal of Medicinal Chemistry 93 (2015) 443–451

Contents lists available at ScienceDirect

European Journal of Medicinal Chemistry

journal homepage: http://www.elsevier.com/locate/ejmech

Original article

Antioxidant activity and inhibition of α-glucosidase by hydroxyl-functionalized 2-arylbenzo[*b*]furans

Jung-Feng Hsieh [a], Wei-Jen Lin [b], Kai-Fa Huang [c], Jiahn-Haur Liao [c], Ming-Jaw Don [b], Chien-Chang Shen [b], Young-Ji Shiao [b], Wen-Tai Li [b, *]

[a] *Department of Food Science, Fu Jen Catholic University, Taipei 24205, Taiwan*
[b] *National Research Institute of Chinese Medicine, Ministry of Health and Welfare, Taipei 11221, Taiwan*
[c] *Institute of Biological Chemistry, Academia Sinica, Taipei 11529, Taiwan*

ARTICLE INFO

Article history:
Received 20 October 2014
Received in revised form
5 February 2015
Accepted 15 February 2015
Available online 16 February 2015

Keywords:
Hydroxyl-functionalized 2-arylbenzo[b]furans
Alpha-glucosidase
Antioxidant
DPPH radical scavenging assay

ABSTRACT

This study synthesized a series of hydroxyl-functionalized 2-arylbenzo[*b*]furans based on the structure of tournefolic acid A and evaluated them for antioxidant and α-glucosidase inhibitory activities. Compounds **5a**, **5e**, and **5n** showed remarkable inhibition of α-glucosidase (IC_{50} values of 1.9–3.0 μM), and they appear to be even more potent than quercetin. A kinetic binding study indicated that compounds **5a** and **5n** used a mechanism of mixed-competition to inhibit α-glucosidase. This study also revealed that compounds **5a** and **5n** bind to either the α-glucosidase or α-glucosidase-4-NPGP complex. Using the crystal structure of the *Saccharomyces cerevisiae* α-glucosidase, the molecular docking study has predicted the binding of compounds **5a** and **5n** to the active site of α-glucosidase through both hydrophobic and hydrogen interactions. A DPPH radical scavenging assay further showed that most hydroxyl-functionalized 2-arylbenzo[*b*]furans possess antioxidant activity. The exception was compound **5p**, which has only one hydroxyl group on the 2-phenyl ring of 2-arylbenzo[*b*]furan. Our results indicate that hydroxyl-functionalized 2-arylbenzo[*b*]furans possess both antidiabetic as well as antioxidant properties.

1. Introduction

Diabetes mellitus is a metabolic disease characterized by hyperglycemia, an abnormal postprandial increase of blood glucose [1,2]. α-Glucosidases are membrane-bound enzymes that help to catalyze the reactions associated with carbohydrate digestion. These enzymes are also required for the cleavage of the α-glycosidic linkage connecting two glucoses or glycoconjugates, the reaction of which leads to the release of glucose [3]. Therefore, the inhibition of α-glucosidases can cause the suppression of carbohydrate ingestion [4,5]. Indeed, for two decades, α-glucosidase inhibitors have been used to treat diabetic patients by lowering the blood glucose levels [6,7]. In addition, α-glucosidase inhibitors have the potential to treat a broad-spectrum of viruses, cancers, and other degenerative diseases, such as nojirimycin and castanospermine [8–11].

Oxidative damage and the increased production of free radicals have been implicated in diabetic complications [12]. Therefore, considerable efforts have been made to develop an anti-diabetic drug that possesses both hypoglycemic and antioxidant properties [13,14]. Catechin and quercetin are polyphenolic compounds found in a variety of plant-based foods and beverages [15,16]. Both of these compounds have excellent antioxidant capacity and are lead compounds in the design of anti-diabetic drugs. The antioxidant properties of catechin and quercetin are due to phenolic structures, and it was found that the electron donating effect of the hydroxyl group is essential [17]. Furthermore, the relatively planar structures of polyphenols have a higher antioxidant capacity. For instance, the relatively planar conformation of quercetin allows for the conjugated π-system of the AC-ring to interact efficiently with the B-ring, which gives quercetin an antioxidant capacity that is higher than that of its nonplanar derivatives [18]. In addition, a number of polyphenols, such as quercetin and epicatechin, have been found to possess both antioxidant properties and inhibit α-glucosidase [19]. The relatively planar structures of catechin derivatives have more pronounced α-glucosidase inhibitory activity than catechin itself [20]. Therefore, planar polyphenols likely have stronger antioxidant and α-glucosidase inhibition activity than

* Corresponding author. National Research Institute of Chinese Medicine, Ministry of Health and Welfare, 155-1, Sec. 2, Linong St., Beitou Distrct, Taipei 11221, Taiwan.
E-mail address: wtli@nricm.edu.tw (W.-T. Li).

http://dx.doi.org/10.1016/j.ejmech.2015.02.024
0223-5234/

non-planar polyphenols, suggesting that planar phenolic structures can improve the therapeutic efficacy of antidiabetic drugs.

Tournefolic acid A, which is characterized by a planar phenolic structure, has been reported to inhibit Cu^{2+}-induced low-density-lipoprotein (LDL) peroxidation, but it has never been reported to inhibit α-glucosidase (Fig. 1) [21]. The planar scaffold of tournefolic acid A, hydroxyl-functionalized 2-arylbenzo[*b*]furan conserves antioxidant activity and may also possess the α-glucosidase inhibition potential. Therefore, we used tournefolic acid A to develop novel antidiabetic agents that contain a planar scaffold of hydroxyl-functionalized 2-arylbenzo[*b*]furan.

In this study, we demonstrate the efficient synthesis of hydroxyl-functionalized 2-arylbenzo[*b*]furan derivatives and report on the antioxidant and α-glucosidase inhibitory effects of these derivatives. We also describe the potential docking model and mechanism underlying enzymatic inhibition by hydroxyl-functionalized 2-arylbenzo[*b*]furans.

2. Results and discussion

2.1. Synthesis

The synthetic strategies for new antioxidants and α-glucosidase inhibitors with the structural scaffold of 2-arylbenzo[*b*]furan are outlined in Schemes 1–3. One-pot palladium-catalyzed coupling of 2-iodophenol with alkynes was utilized to efficiently construct the 2-arylbenzo[*b*]furan core structure (Scheme 1). First, phenylacetylene **2** was synthesized via a two-step reaction, as follows. Substituted benzaldehyde was treated with carbon tetrabromide to yield 1,1-dibromo-1-alkene **1**. This interim compound was then debrominated using *n*-butyl lithium, which generated phenylacetylene **2**, as shown in Scheme 1 [22]. Subsequently, one-pot palladium-catalyzed coupled phenylacetylene **2** with 2-iodo-6-methoxyphenol **3** using palladium catalysis, yielded 2-arylbenzo[*b*]furan **4a** [23]. To synthesize hydroxyl-functionalized 2-arylbenzo[*b*]furan **5a**, deprotection of three methoxy groups on 2-arylbenzo[*b*]furan **4a** was performed under strong acid conditions using boron tribromide. However, attempts to carry out one-pot palladium-catalyzed coupled reaction to obtain some halo-substituted 2-arylbenzo[*b*]furans were unsuccessful; therefore, a four-step procedure involving the Wittig reaction was employed to synthesize those compounds. Specifically, 2-arylbenzo[*b*]furan **4b** was prepared using the Wittig reaction to convert substituted phosphonium ylide **7** and *o*-vanillin into stilbene **8**. This was followed by cyclization in a basic iodine solution, as shown in Scheme 2. Boron tribromide was used to deprotect the methoxy-substituted 2-arylbenzo[*b*]furan **4b** in a similar fashion, and compound **4b** was then converted to the desired hydroxyl-functionalized 2-arylbenzo[*b*]furan **5b**. Bromo substituted 2-arylbenzo[*b*]furan **4b** was coupled with ethyl acrylate though a palladium-catalyzed Heck coupling reaction to produce (*E*)-ethyl acrylate substituted 2-arylbenzo[*b*]furan **9a**. The methoxy groups were removed from compound **9a** using the same boron tribromide treatment procedure to obtain (*E*)-ethyl acrylate substituted hydroxyl-functionalized 2-arylbenzo[*b*]furan **5p**.

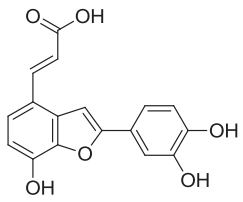

Fig. 1. Chemical structure of tournefolic acid A.

2.2. Inhibition of α-glucosidase

All of the synthesized 2-arylbenzo[*b*]furans (Table 1) were evaluated for α-glucosidase inhibition activity in accordance with standard procedures [24]. For this analysis, quercetin and resveratrol were used for comparison purposes. The IC_{50} values, indicating the strength of α-glucosidase inhibition by 2-arylbenzo[*b*]furans, are summarized in Table 2. Compounds **5a**, **5e**, and **5n** were shown to be potent α-glucosidase inhibitors with IC_{50} values of 1.9–3.0 μM. This is 2- to 3-times more potent than quercetin (IC_{50} = 6.6 μM), a known α-glucosidase inhibitor. Indeed, most of the hydroxyl-functionalized 2-arylbenzo[*b*]furans (except **5g**, **5m**, and **5p**) presented with potent inhibitory activity with IC_{50} values below 10 μM. Nevertheless, hydroxyl-functionalized 2-arylbenzo[*b*]furans **5l** and **5m**, with an (*E*)-ethyl acrylate substitution, only showed modest activity with IC_{50} values of 8.9 and 23.8 μM, respectively. Compound **5p**, which has only one hydroxyl group on the 2-phenyl ring of 2-arylbenzo[*b*]furan, presented with potency similar to that of the reference inhibitor resveratrol. Moreover, compounds **5b**, **5c**, **5f**, **5h**, and **5k**, which have a catechol ring on the 2-position of 2-arylbenzo[*b*]furan, showed similar levels of inhibitory activity. In a comparison of compounds **5a** and **5b**, the bromo substituent on the catechol ring of 2-arylbenzo[*b*]furan was found to confer an increase in inhibitory activity on par with compounds **5e** and **5i**. However, compounds **5f** and **5k**, which possess a bromo substituent on the 4 and 5-position of 2-arylbenzo[*b*]furan, presented with potency similar to that of compound **5b**. Finally, the inhibitory activity of the pyrogallol ring on the 2-position of benzo[*b*]furan **5e** is superior to that of the catechol **5k** and 4-hydroxyphenyl **5p** groups. The relative inhibitory strengths of compounds considered by this study were as follows: pyrogallol > catechol > 4-hydroxyphenyl. The methoxy-substituted 2-arylbenzo[*b*]furans **4a**, **4b**, **4c**, and **9a** were inactive at the highest tested concentration (>100 μM).

2.3. Evaluation of antioxidant activities

The antioxidant activity of synthesized 2-arylbenzo[*b*]furans was evaluated using DPPH radical scavenging assays [25]. This widely-used method determines antioxidant activity by measuring the hydrogen donating ability of the compound being studied. The IC_{50} values are displayed in Table 3. Methoxy-substituted 2-arylbenzo[*b*]furans (i.e. compounds **4a**, **4b**, **4c**, and **9a**) did not reveal any DPPH radical scavenging activity (IC_{50} > 100 μM). However, most of the hydroxyl-functionalized 2-arylbenzo[*b*]furans (i.e. compounds **5a**-**5o**, but not **5p**) demonstrated radical scavenging activity in the micromolar range, and a number of these were also potent in the low micromolar range. A comparison of compounds with the pyrogallol ring **5e**, catechol ring **5k**, and 4-hydroxyphenyl ring **5p** on the 2-position of 2-arylbenzo[*b*]furan revealed that these compounds possess the same order of radical scavenging activity as their α-glucosidase inhibition activity, which is pyrogallol > catechol > 4-hydroxyphenyl. In addition, compounds **5e**, **5i**, and **5j**, which contain a pyrogallol ring on the 2-position of 2-arylbenzo[*b*]furan, demonstrated comparable DPPH free radical scavenging activities; however, they were 2-fold less potent than quercetin. Finally, the free radical scavenging ability of (*E*)-ethyl acrylate substituents **5l** and **5m** was slightly better than that of bromo substituents **5c**, **5f**, and **5k**.

2.4. Mode of α-glucosidase inhibition by hydroxyl-functionalized 2-arylbenzo[b]furans

Inhibition kinetics of hydroxyl-functionalized 2-arylbenzo[*b*]furans were determined by conducting a Lineweaver–Burk plot

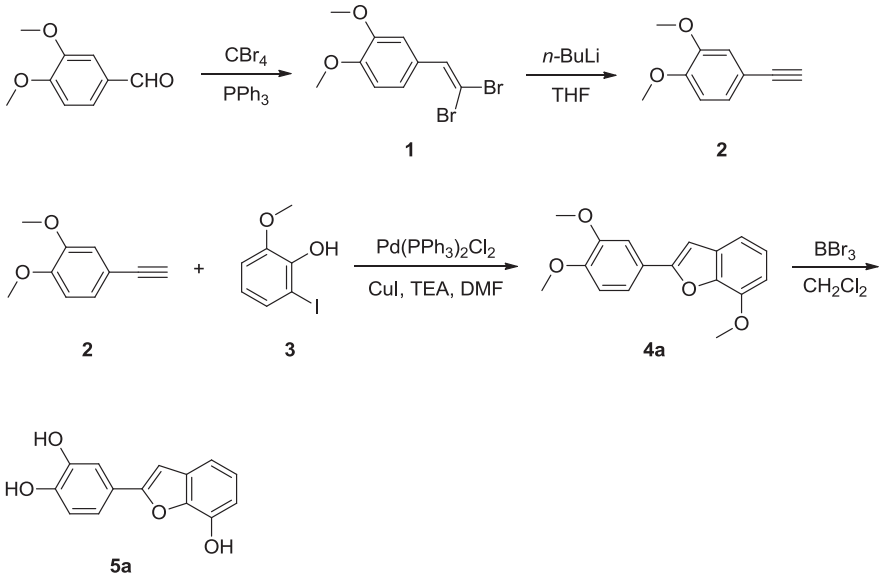

Scheme 1. Synthesis of compound **5a** from palladium-catalyzed coupled phenylacetylene **2** with 2-iodo-6-methoxyphenol **3**.

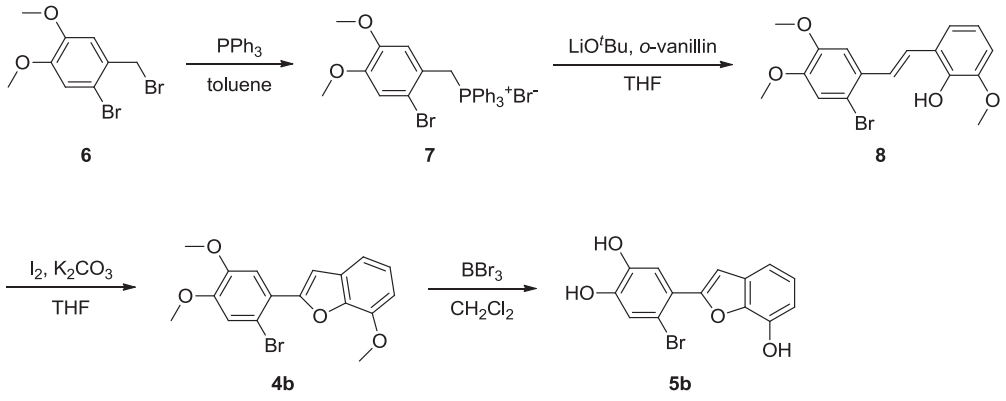

Scheme 2. Synthesis of compound **5b** via Wittig reaction and cyclization reactions.

analysis on compounds **5a** and **5n**, as shown in Fig. 2 [24]. In this figure, the concentrations of 1/(4-NPGP) are displayed on the X-axis, and 1/V values obtained from the Lineweaver–Burk plot are shown along the Y-axis. The plots did not intersect either the X- or Y-axis, suggesting that both **5a** and **5n** are mixed-type mode inhibitors with respect to 4-NPGP for α-glucosidase. We also examined Dixon plots of how compounds **5a** and **5n** affect α-glucosidase. As shown in Fig. 3, these plots further confirm that compounds **5a** and **5n** are mixed-type α-glucosidase inhibitors. The *Ki* values of **5a** and **5n** were 4.21 ± 0.03 μM and 3.19 ± 0.1 μM, respectively, while the *Ki′* values of these compounds were 13.66 ± 1.38 μM and 11.81 ± 1.08 μM, respectively. *Ki* is the equilibrium constant for the inhibitor binding to α-glucosidase, and *Ki′* is the equilibrium constant for the inhibitor binding to the α-glucosidase-4-NPGP complex. Previous studies have reported that in a reversible mixed-competitive inhibition reaction, the *Ki* values are usually smaller than the *Ki′* values, and the results from this current study are in strong agreement with those findings. This indicates that the inhibitor-enzyme binding affinity exceeds the binding affinity of the inhibitor-enzyme-substrate complex and compounds **5a** and **5n** are mixed-competitive inhibitors of α-glucosidase. The binding sites and mechanism underlying inhibition have yet to be determined; however, the result of mixed-competitive inhibition against α-glucosidase suggests that compounds **5a** and **5n** may bind to

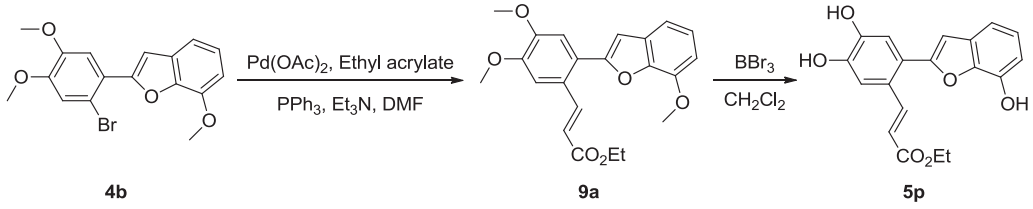

Scheme 3. Synthesis of compound **5p** via palladium-catalyzed Heck coupling reaction from bromo substituted 2-arylbenzo[*b*]furan **4b**.

Table 1
2-Arylbenzo[*b*]furans prepared via one-pot palladium-catalyzed or Wittig reactions.

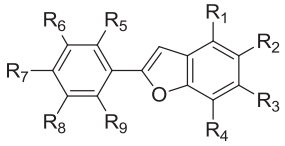

Compd	R_1	R_2	R_3	R_4	R_5	R_6	R_7	R_8	R_9
4a	H	H	H	OCH_3	H	OCH_3	OCH_3	H	H
4b	H	H	H	OCH_3	H	OCH_3	OCH_3	H	Br
4c	H	Br	H	OCH_3	H	OCH_3	OCH_3	OCH_3	H
5a	H	H	H	OH	H	H	OH	OH	H
5b	H	H	H	OH	Br	H	OH	OH	H
5c	H	H	H	H	Br	H	OH	OH	H
5d	H	H	H	H	Br	OH	OH	OH	H
5e	H	Br	H	OH	H	OH	OH	OH	H
5f	Br	H	H	OH	H	OH	OH	H	H
5g	Br	H	H	OH	Br	OH	OH	OH	H
5h	Br	H	H	OH	H	OH	OH	H	Br
5i	H	H	H	OH	H	OH	OH	OH	H
5j	H	H	H	H	H	OH	OH	OH	H
5k	H	Br	H	OH	H	OH	OH	H	H
5l	(*E*) −CH═$CHCO_2Et$	H	H	OH	H	OH	OH	H	H
5m	H	(*E*) −CH═$CHCO_2Et$	H	OH	H	OH	OH	H	H
5n	H	(*E*) −CH═$CHCO_2Et$	H	OH	H	OH	OH	OH	H
5o	H	H	H	OH	H	OH	OH	H	(*E*) −CH═$CHCO_2Et$
5p	H	Br	H	OH	H	H	OH	H	H
9a	H	H	H	OCH_3	H	OCH_3	OCH_3	H	(*E*) −CH═$CHCO_2Et$

either α-glucosidase or the α-glucosidase-4-NPGP complex.

2.5. Molecular modeling

The docking experiments were performed base on the maltose binding model of *Saccharomyces cerevisiae* α-glucosidase, as shown in Fig. 4 [26]. There are three catalytic acidic residues in the active site of α-glucosidase and they are Asp 215, Glu 277, and Asp 352. Both binding models of compounds **5a** and **5n** showed that Asp 215 is involved in the interactions between the compound and enzyme. For compound **5a**, there are two residues (Arg 213 and Asp 215) formed two hydrogen bonds with the compound. One catalytic acidic residue, Asp 215, is involved in the binding of compound **5a**. In a competitive inhibitor maltose binding model, Arg 213 also formed hydrogen bond with maltose. Compound **5a** and maltose may show similar binding properties with α-glucosidase. For compound **5n**, three residues (Asp 69, Asp 215, and Arg 442) formed three hydrogen bonds with the compound. In addition to the catalytic acidic residue (Asp 215), Asp 69 and Arg 442 were shown to interact with maltose [26]. Compound **5n** may occupy the glucose binding site of α-glucosidase through hydrogen bonding with these three residues. The moiety −CH═$CHCO_2Et$ of **5n** is extend into the pocket formed by Gln 22, Trp 58, Phe 301, and Tyr 387. Hydrophobic interactions may be involved in the binding of compound **5n**.

3. Conclusions

An ideal anti-diabetic drug should possess both hypoglycemic and antioxidant properties and be free from adverse side effects. This study prepared a series of hydroxyl-functionalized 2-arylbenzo[*b*]furan compounds from the core structure of tournefolic acid A using one-pot palladium-catalyzed coupling methods. The synthesized 2-arylbenzo[*b*]furans were evaluated for α-glucosidase inhibition and antioxidant activity. A DPPH radical scavenging assay revealed that most of these compounds possess antioxidant properties. Some of the hydroxyl-functionalized 2-arylbenzo[*b*]furans also showed remarkable inhibitory activity

Table 2
α-Glucosidase inhibitory activity of 2-arylbenzo[*b*]furans.

Compound	α-Glucosidase IC_{50} (μM)[a]	Compound	α-Glucosidase IC_{50} (μM)[a]
Resveratrol	31.1 ± 0.8[b]	**5g**	12.4 ± 0.7
Quercetin	6.6 ± 0.4[c]	**5h**	6.4 ± 0.8
4a	>100	**5i**	9.2 ± 0.2
4b	>100	**5j**	8.2 ± 1.7
4c	>100	**5k**	7.5 ± 0.8
5a	1.9 ± 0.2	**5l**	8.9 ± 0.6
5b	7.1 ± 0.5	**5m**	23.8 ± 0.6
5c	7.7 ± 1.6	**5n**	2.0 ± 0.4
5d	8.5 ± 0.7	**5o**	5.5 ± 0.5
5e	3.0 ± 0.4	**5p**	29.8 ± 3.2
5f	6.4 ± 0.5	**9a**	>100

[a] IC_{50} values represent as mean ± SD of three determinations.
[b] Reported IC_{50} = 27.9 μM.
[c] Reported IC_{50} = 5.3 μM.

Table 3
DPPH radical scavenging activity of 2-arylbenzo[*b*]furans.

Compound	DPPH IC_{50} (μM)[a]	Compound	DPPH IC_{50} (μM)[a]
Resveratrol	63.5 ± 5.5[b]	**5g**	19.4 ± 2.8
Quercetin	6.0 ± 0.7[c]	**5h**	7.8 ± 1.6
4a	>100	**5i**	12.8 ± 0.7
4b	>100	**5j**	10.8 ± 1.1
4c	>100	**5k**	28.6 ± 3.4
5a	18.5 ± 2.5	**5l**	16.8 ± 1.2
5b	20.6 ± 1.9	**5m**	25.4 ± 3.1
5c	33.8 ± 2.8	**5n**	11.7 ± 1.8
5d	18.0 ± 1.7	**5o**	26.2 ± 2.8
5e	14.6 ± 2.1	**5p**	>100
5f	18.4 ± 2.7	**9a**	>100

[a] IC_{50} values represent as mean ± SD of three determinations.
[b] Reported IC_{50} = 38.0 μM.
[c] Reported IC_{50} = 9.1 μM.

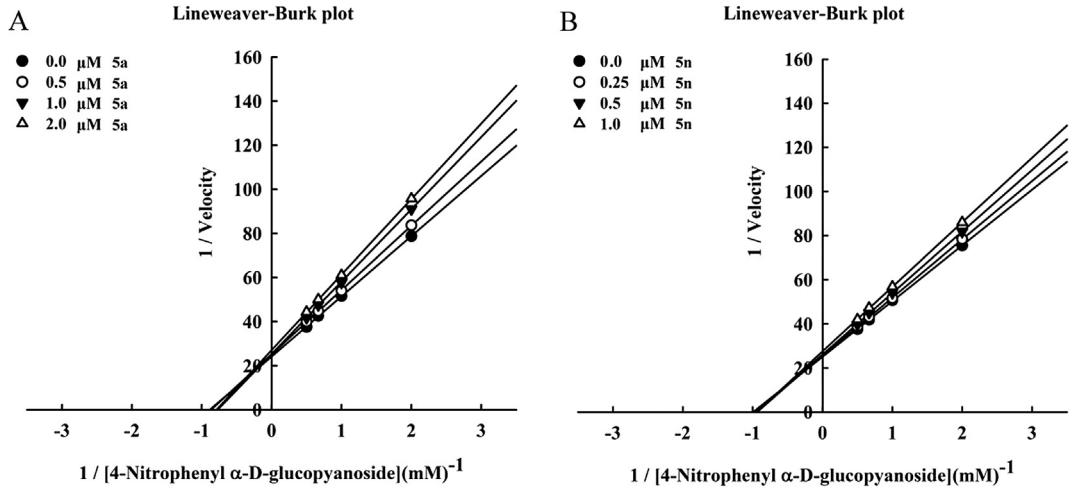

Fig. 2. Linweave-Burk analysis of compounds **5a** (A) and **5n** (B). The **5a** (A) concentrations were 0.0 μM (●), 0.5 μM (○), 1.0 μM (▼) and 2.0 μM (△). The **5n** (B) concentrations were 0.0 μM (●), 0.25 μM (○), 0.5 μM (▼) and 1.0 μM (△).

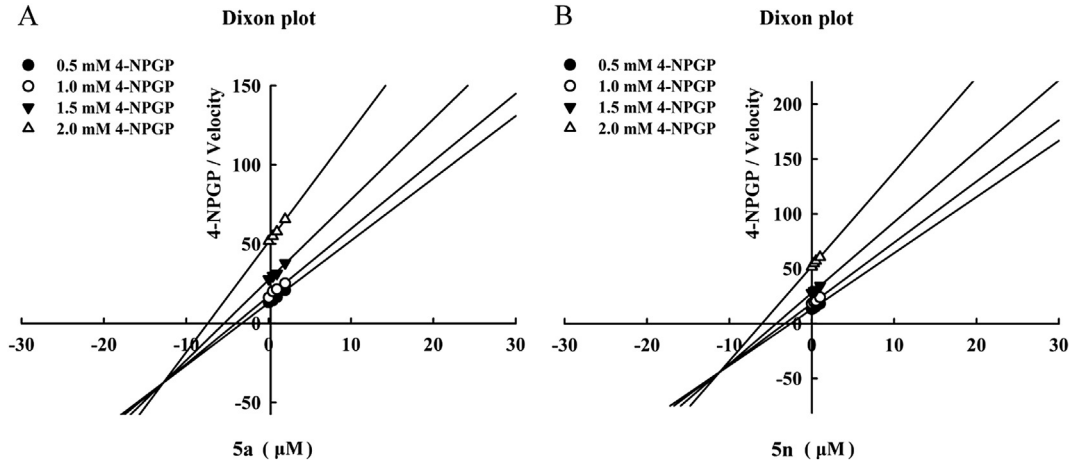

Fig. 3. Dixon plots of compounds **5a** (A) and **5n** (B). The 4-NPGP concentrations were 0.5 mM (●), 1.0 mM (○), 1.5 mM (▼) and 2.0 mM (△).

against α-glucosidase with potency exceeding that of quercetin. Further investigation of binding kinetics indicated that the mechanism of α-glucosidase inhibition by compounds **5a** and **5n** was mixed-competitive. This suggests that the hydroxyl-functionalized 2-arylbenzo[*b*]furans may bind to either the α-glucosidase or α-glucosidase-4-NPGP complex. Furthermore the docking study has predicted that compounds **5a** and **5n** bind to the active site of the *S. cerevisiae* α-glucosidase through both hydrophobic and hydrogen interactions. Compound **5a** and maltose may have binding properties that are similar to α-glucosidase, and compound **5n** may occupy the glucose binding site of α-glucosidase through hydrogen bonding with the three amino acid residues of Asp 69, Asp 215, and Arg 442. Taken together, our results suggest that hydroxyl-functionalized 2-arylbenzo[*b*]furans **5a** and **5n** are promising candidates for the further development of diabetes treatments.

4. Experimental section

4.1. Chemistry synthesis

All reactions were conducted in dried glassware under an oven at 120 °C overnight and cooled in a desiccator. All reagents were used as received from commercial suppliers unless otherwise stated. Dichloromethane (DCM) and *N*,*N*′-dimethylformamide (DMF) were dried over calcium hydride for 48 h prior to distillation. Tetrahydrofuran (THF) was distilled from sodium/benzophenone ketyl under nitrogen. The proton NMR spectra were obtained on Bruker Avance 400 (400 MHz), Varian Unity Inova 500 (500 MHz) and Varian VNMRS600 (600 MHz) spectrometers. All NMR chemical shifts were reported as δ values in parts per million (ppm), and coupling constants (J) were given in hertz (Hz). The splitting pattern abbreviations are as follows: s, singlet; d, doublet; t, triplet; q, quartet; br, broad; m, unresolved multiplet due to the field strength of the instrument; dd, doublet of doublet; dt, doublet of triplet; and ddd, doublet of doublet of doublet. Melting points were measured on a Yanaco MP-S3 micro melting point apparatus and are uncorrected. Fourier transform infrared spectra were collected with an Avatar 320 spectrometer. Mass spectra were carried out on ThermoQuest Finnigan and Microsaic 4000MiD mass spectrometers. Purification was performed using preparative separations in flash column chromatography (Merck silica gel 60, particle size of 230–400 mesh). Analytical TLC was carried out on precoated plates (Merck silica gel 60, F254). The compounds analyzed on the TLC plates were visualized using a UV light, I_2 vapor, or basic aqueous potassium permanganate ($KMnO_4$) with heating.

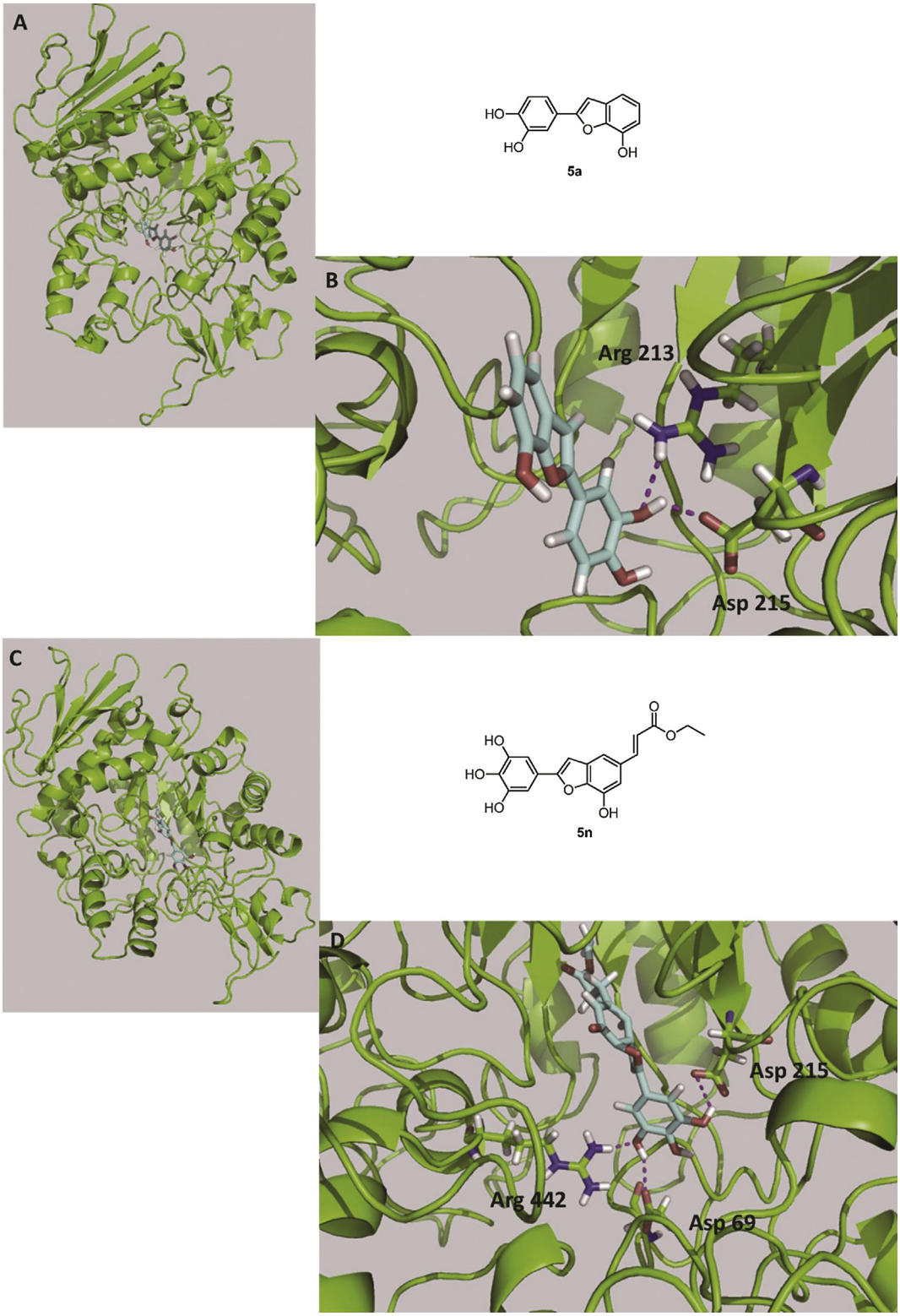

Fig. 4. Proposed structure models of compound-α-glucosidase complex. (A) 3D-structural model of *S. cerevisiae* α-glucosidase bound to compound **5a**. The 3D-structural model of α-glucosidase is shown in green. (B) A close-up view of the compound **5a** molecule bound in the active site of *S. cerevisiae* α-glucosidase. Residues that may be involved in the interactions of compound binding are drawn with a stick model and shown in different colors. The possible hydrogen-bond interactions are indicated with dashed lines (purple). (C) The 3D-structural model of *S. cerevisiae* α-glucosidase bound to compound **5n**. (D) A close-up view of the compound **5n** molecule bound in the active site of *S. cerevisiae* α-glucosidase. Residues that may be involved in the interactions of compound binding are drawn with stick model and shown in different colors. The possible hydrogen-bond interactions are indicated with dashed lines (purple). (For interpretation of the references to colour in this figure legend, the reader is referred to the web version of this article.)

*4.1.1. General procedure for synthesis of 2-(3,4-dimethoxyphenyl) -7-methoxybenzofuran (**4a**) via palladium-catalyzed coupled reaction*

A solution of 4-ethynyl-1,2-dimethoxybenzene **2** (105 mg, 0.65 mmol), 2-iodo-6-methoxyphenol **3** (135 mg, 0.54 mmol), bis(triphenylphosphine) palladium(II) chloride (19 mg, 0.027 mmol), copper(I) iodide (5 mg, 0.027 mmol) and triethylamine (0.15 mL) in *N,N′*-dimethylformamide (5 mL) under nitrogen atmosphere was heated at 70 °C for 24 h until complete by TLC. The reaction mixture was quenched with water and extracted with ethyl acetate. The organic layers were combined, dried over with $MgSO_4$ and concentrated. The residue was purified by column chromatography to give the 2-arylbenzo[*b*]furan **4a** (79 mg, 52%) as a white solid. ^{1}H NMR (500 MHz, $CDCl_3$): 7.45 (dd, J = 8.0, 2.0 Hz, 1H), 7.36 (d, J = 2.0 Hz, 1H), 7.13 (s, 1H), 7.10 (t, J = 8.0 Hz, 1H), 6.90 (d, J = 8.0 Hz, 1H), 6.88 (s, 1H), 6.77 (dd, J = 8.0, 2.0 Hz, 1H), 4.02 (s, 3H), 3.97 (s, 3H), 3.90 (s, 3H).^{13}C NMR (125 MHz, $CDCl_3$): 156.1, 149.5, 149.1, 145.1, 143.8, 131.1, 123.5, 123.4, 118.1, 113.0, 111.2, 108.2, 106.3, 100.4, 56.0, 55.9. ESMS *m*/*z*: 307.3 $(M + 23)^+$.

*4.1.2. General procedure for the synthesis of (E)-2-(2-bromo-4,5-dimethoxystyryl) -6-methoxyphenol (**8**) via Wittig reaction*

To a solution of phosphorus ylide **7** (297 mg, 0.52 mmol) in THF (20 mL) was cooled to 0 °C under nitrogen and lithium *tert*-butoxide (83 mg, 1.04 mmol) was added portionwise. The mixture was stirred at 0 °C for 30 min. A solution of 6-bromo-2-hydroxy-3-methoxybenzaldehyde (79 mg, 0.52 mmol) in THF (5 mL) was added dropwise at 0 °C and the reaction mixture was warmed up to room temperature and stirred for 24 h. Sat'd aqueous NH_4Cl solution was added to the reaction mixture and extracted with EtOAc (15 mL × 3). The combined organic layers were washed with brine, dried with $MgSO_4$, filtered and concentrated. The residue was purified by column chromatography to yield **8** (97 mg, 51%) as a white solid. ^{1}H NMR (500 MHz, $CDCl_3$): 7.00 (s, 1H), 6.75 (d, J = 12.0, 1H), 6.72-6.65 (m, 2H), 6.60 (t, J = 8.0 Hz, 1H), 5.77 (s, 1H), 3.86 (s, 3H), 3.84 (s, 3H), 3.43 (s, 3H). ^{13}C NMR (125 MHz, $CDCl_3$): 148.8, 147.6, 146.6, 143.5, 129.6, 129.5, 124.8, 123.0, 122.1, 119.1, 115.0, 114.4, 113.2, 109.5, 56.0, 56.0, 55.6. ESMS *m*/*z*: 388.7 $(M + 23)^+$.

*4.1.3. General procedure for the synthesis of 2-(2-bromo-4,5-dimethoxyphenyl)-7-methoxybenzofuran (**4b**)*

To a solution of (*E*)-2-(2-bromo-4,5- dimethoxystyryl)-6-methoxyphenol **8** (250 mg, 0.68 mmol) in 15 mL of THF was mixed with potassium carbonate (568 mg, 4.1 mmol) and iodine (1.04 g, 4.1 mmol). The mixture was stirred at room temperature for 3 h until complete by TLC. Sat'd $NaHSO_3$ aqueous solution was added to the solution, and the mixture was extracted with ethyl acetate. The organic layers were combined and dried over $MgSO_4$. The residue was purified by flash column chromatography to afford the title compound (206 mg, 83%) as a yellowish solid. Mp = 106–109 °C. IR νmax: 3439, 2953, 1511, 1254, 1180 cm^{-1}. ^{1}H NMR (500 MHz, $CDCl_3$): 7.44 (s, 1H), 7.38 (s, 1H), 7.20 (d, J = 8.0 Hz, 1H), 7.15 (t, J = 8.0 Hz, 1H), 7.12 (s, 1H), 6.80 (d, J = 8.0 Hz, 1H), 4.02 (s, 3H), 3.95 (s, 3H), 3.90 (s, 3H). ^{13}C NMR (125 MHz, $CDCl_3$): 153.4, 149.4, 148.3, 145.2, 143.4, 130.7, 123.6, 123.4, 116.6, 113.6, 112.2, 111.6, 106.7, 106.3, 56.2, 56.1, 56.0. ESMS *m*/*z*: 385.2 $(M + 23)^+$, 747.2 $(2M + 23)^+$.

*4.1.3.1. 5-Bromo-7-methoxy-2-(3,4,5-trimethoxyphenyl)benzofuran (**4c**).* Yield: 81%. Amorphous powder. IR νmax: 3441, 2957, 1531, 1251, 1132 cm^{-1}. ^{1}H NMR (500 MHz, $CDCl_3$): 7.28 (d, J = 1.5 Hz, 1H), 7.05 (s, 1H), 6.89 (d, J = 1.5 Hz, 1H), 6.86 (s, 1H), 4.01 (s, 3H), 3.94 (s, 6H), 3.88 (s, 3H). ^{13}C NMR (125 MHz, $CDCl_3$): 157.0, 153.6, 145.5, 143.0, 139.1, 125.4, 116.0, 115.8, 110.1, 102.5, 100.7, 61.0, 56.3, 56.2, 29.7. ESMS *m*/*z*: 393.2 $(M + 1)^+$, 395.2 $(M + 1)^+$, 415.2 $(M + 23)^+$, 417.2 $(M + 23)^+$.

*4.1.4. General procedure for the synthesis of 4-bromo-5-(7-hydroxybenzofuran -2-yl)benzene-1,2-diol (**5b**)*

To a solution of **4b** (200 mg, 0.55 mmol) in dry dichloromethane (15 mL) at −60 °C under N_2 was added BBr_3 (0.48 ml, 4.96 mmol) dropwise. The reaction mixture was then allowed to warm up to −40 °C and stirred for another 2 h until complete by TLC. The reaction was carefully mixed with addition of sat'd aqueous $NaHCO_3$ (20 mL) at 0 °C and stirred for 30 min. This mixture was extracted with ethyl acetate twice (15 mL × 2) and the organic portion was combined, washed further with brine, and dried with $MgSO_4$. The residue was filtered, concentrated and purified by column chromatography to yield **5b** as an off-white solid (122 mg, 69%). Mp = 205–210 °C. IR νmax: 3253, 1596, 1489, 1174 cm^{-1}. ^{1}H NMR (500 MHz, CD_3OD): 7.43 (s, 1H), 7.30 (s, 1H), 7.09 (s, 1H), 7.06 (dd, J = 7.8, 1.2 Hz, 1H), 7.00 (t, J = 7.8 Hz, 1H), 6.72 (dd, J = 7.8, 1.2 Hz, 1H). ^{13}C NMR (125 MHz, CD_3OD): 154.8, 148.0, 146.3, 144.1, 143.4, 132.2, 124.6, 123.6, 121.5, 117.2, 113.2, 111.5, 110.6, 106.5. ESMS *m*/*z*: 321.1 $(M - 1)^-$.

*4.1.4.1. 4-(7-Hydroxybenzofuran-2-yl)benzene-1,2-diol (**5a**).* Yield: 72%. Mp = 149–152 °C. IR νmax: 3253, 1596, 1489, 1206, 1069 cm^{-1}. ^{1}H NMR (600 MHz, CD_3OD): 7.33 (d, J = 2.0 Hz, 1H), 7.26 (dd, J = 8.5, 2.0 Hz, 1H), 6.99 (d, J = 7.5 Hz, 1H), 6.98 (dd, J = 15.0, 8.0 Hz, 1H), 6.84 (d, J = 8.0 Hz, 1H), 6.84 (s, 1H), 6.88 (dd, J = 7.5, 2.0 Hz, 1H). ^{13}C NMR (150 MHz, CD_3OD): 157.6, 147.3, 146.6, 144.6, 143.3, 132.8, 124.5, 124.0, 118.2, 116.6, 113.1, 112.8, 111.0, 100.5. ESMS *m*/*z*: 241.4 $(M - 1)^-$.

*4.1.4.2. 4-(Benzofuran-2-yl)-5-bromobenzene-1,2-diol (**5c**).* Yield: 64%. Mp = 111–113 °C. IR νmax: 3333, 1614, 1506, 1256 cm^{-1}. ^{1}H NMR (500 MHz, $CDCl_3$): 7.59 (d, J = 7.5 Hz, 1H), 7.48 (s, 1H), 7.47 (dd, J = 7.5, 0.5 Hz, 1H), 7.40 (d, J = 0.5 Hz, 1H), 7.28 (dt, J = 7.5, 1.0 Hz, 1H), 7.22 (dt, J = 7.5, 1.0 Hz, 1H), 7.21 (s, 1H), 5.59 (s, 1H), 5.38 (s, 1H). ^{13}C NMR (125 MHz, $CDCl_3$): 154.0, 152.9, 144.5, 142.8, 128.9, 124.5, 122.9, 121.2, 120.8, 116.1, 111.4, 110.9, 105.9. ESMS *m*/*z*: 305.2 $(M - 1)^-$.

*4.1.4.3. 5-(Benzofuran-2-yl)-4-bromobenzene-1,2,3-triol (**5d**).* Yield: 62%. Mp = 159–162 °C. IR νmax: 3419, 1613, 1507, 1452, 1187 cm^{-1}. ^{1}H NMR (600 MHz, CD_3OD): 7.58 (d, J = 7.2 Hz, 1H), 7.45 (dd, J = 7.8, 0.6 Hz, 1H), 7.31 (d, J = 0.6 Hz, 1H), 7.26 (dt, J = 7.2, 1.2 Hz, 1H), 7.20 (dt, J = 7.2, 1.2 Hz, 1H), 7.01 (s, 1H). ^{13}C NMR (150 MHz, CD_3OD): 155.8, 155.4, 146.1, 145.2, 136.2, 130.4, 125.2, 123.6, 123.0, 122.0, 111.6, 109.3, 100.9. ESMS *m*/*z*: 321.0 $(M - 1)^-$.

*4.1.4.4. 5-(5-Bromo-7-hydroxybenzofuran-2-yl)benzene-1,2,3-triol (**5e**).* Yield: 59%. Mp = 224–227 °C. IR νmax: 3445, 1646, 1445, 1314, 1197 cm^{-1}. ^{1}H NMR (500 MHz, CD_3OD): 7.14 (d, J = 2.0 Hz, 1H), 6.90 (s, 2H), 6.80 (d, J = 2.0 Hz, 1H), 6.78 (s, 1H). ^{13}C NMR (125 MHz, CD_3OD): 159.1, 147.3, 144.2, 143.6, 135.9, 134.2, 122.4, 116.6, 115.2, 114.1, 105.6, 100.1. ESMS *m*/*z*: 337.1 $(M - 1)^-$.

*4.1.4.5. 4-(4-Bromo-7-hydroxybenzofuran-2-yl)benzene-1,2-diol (**5f**).* Yield: 67%. Mp = 82–86 °C. IR νmax: 3220, 2924, 1486, 1186 cm^{-1}. ^{1}H NMR (400 MHz, CD_3OD): 7.33 (d, J = 2.5 Hz, 1H), 7.30 (d, J = 8.0 Hz, 1H), 7.12 (d, J = 8.0 Hz, 1H), 6.85 (d, J = 8.5 Hz, 1H), 6.83 (s, 1H), 6.61 (d, J = 8.5 Hz, 1H). ^{13}C NMR (125 MHZ, CD_3OD): 158.5, 148.0, 146.8, 144.3, 143.2, 133.4, 127.1, 123.2, 118.5, 116.7, 113.2, 112.3, 103.1, 100.2. ESMS *m*/*z*: 321.2 $(M - 1)^-$.

*4.1.4.6. 4-Bromo-5-(4-bromo-7-hydroxybenzofuran-2-yl)benzene-1,2,3-triol (**5g**).* Yield: 55%. Mp = 171–174 °C. IR νmax: 3378, 1609,

1486, 1294, 1190 cm^{-1}. ^1H NMR (600 MHz, CD_3OD): 7.24 (s, 1H), 7.15 (d, J = 7.8 Hz, 1H), 7.07 (s, 1H), 6.66 (d, J = 7.8 Hz, 1H), 4.60 (br). ^{13}C NMR (150 MHz, CD_3OD): 156.2, 146.2, 145.2, 143.9, 143.2, 136.6, 132.7, 127.1, 122.3, 112.7, 109.5, 106.2, 103.4, 101.0. ESMS m/z: 415.0 $(M - 1)^-$.

*4.1.4.7. 4-Bromo-5-(4-bromo-7-hydroxybenzofuran-2-yl)benzene-1,2-diol (**5h**).* Yield: 61%. Mp = 210–214 °C. IR νmax: 3260, 1592, 1484, 1277, 1199 cm^{-1}. ^1H NMR (500 MHz, CD_3OD): 7.43 (s, 1H), 7.26 (s, 1H), 7.13 (d, J = 8.4 Hz, 1H), 7.11 (s, 1H), 6.66 (d, J = 8.4 Hz, 1H), 5.03 (br). ^{13}C NMR (125 MHz, CD_3OD): 155.6, 148.5, 146.4, 143.9, 143.3, 132.7, 127.2, 122.9, 121.6, 117.2, 112.8, 110.8, 106.0, 103.4. ESMS m/z: 399.0 $(M - 1)^-$.

*4.1.4.8. 5-(7-Hydroxybenzofuran-2-yl)benzene-1,2,3-triol (**5i**).* Yield: 67%. Mp = 200–203 °C. IR νmax: 3332, 1747, 1595, 1447, 1310, 1192 cm^{-1}. ^1H NMR (500 MHz, CD_3OD): 7.24 (s, 1H), 7.15 (d, J = 7.8 Hz, 1H), 7.07 (s, 1H), 6.66 (d, J = 7.8 Hz, 1H), 4.60 (br). ^{13}C NMR (125 MHz, CD_3OD): 156.2, 146.2, 145.2, 143.9, 143.2, 136.6, 132.7, 127.1, 122.3, 112.7, 109.5, 106.2, 103.4, 101.0. ESMS m/z: 257.2 $(M - 1)^-$.

*4.1.4.9. 5-(Benzofuran-2-yl)benzene-1,2,3-triol (**5j**).* Yield: 68%. Mp = 187–188 °C. IR νmax: 3386, 1612, 1522, 1453, 1188 cm^{-1}. ^1H NMR (600 MHz, CD_3OD): 7.51 (dd, J = 7.2, 1.2 Hz, 1H), 7.43 (dd, J = 7.2, 1.2 Hz, 1H), 7.20 (dt, J = 7.2, 1.2 Hz, 1H), 7.16 (dt, J = 7.2, 1.2 Hz, 1H), 6.89 (s, 2H), 6.85 (d, J = 1.2 Hz, 1H). ^{13}C NMR (125 MHz, CD_3OD): 158.0, 155.9, 147.3, 135.6, 131.0, 124.6, 123.8, 122.8, 121.5, 111.6, 105.3, 100.2. ESMS m/z: 241.2 $(M - 1)^-$.

*4.1.4.10. 4-(5-Bromo-7-hydroxybenzofuran-2-yl)benzene-1,2-diol (**5k**).* Yield: 51%. Mp = 221–224 °C. IR νmax: 3231, 2925, 1615, 1446, 1249, 1203 cm^{-1}. ^1H NMR (400 MHz, CD_3OD): 7.30 (d, J = 2.0 Hz, 1H), 7.25 (dd, J = 8.5, 2.0 Hz, 1H), 7.14 (d, J = 2.0 Hz, 1H), 6.84 (d, J = 8.5 Hz, 1H), 6.82 (s, 1H), 6.80 (d, J = 2.0 Hz, 1H). ^{13}C NMR (125 MHz, CD_3OD): 159.0, 147.8, 146.7, 144.2, 143.6, 134.2, 123.4, 118.4, 116.7, 116.6, 115.2, 114.1, 113.2, 100.0. ESMS m/z: 321.1 $(M - 1)^-$.

*4.1.4.11. (E)-Ethyl 3-(2-(3,4-dihydroxyphenyl)-7-hydroxybenzofuran-4-yl) acrylate (**5l**).* Yield: 53%. Mp = 156–160 °C. IR νmax: 3408, 1678, 1613, 1506, 1269, 1177 cm^{-1}. ^1H NMR (500 MHz, CD_3OD): 7.84 (d, J = 16.0 Hz, 1H), 7.36 (d, J = 2.0, 1H), 7.32 (dd, J = 8.0, 2.0 Hz, 1H), 7.27 (d, J = 8.0 Hz, 1H), 7.12 (s, 1H), 6.85 (d, J = 8.5 Hz, 1H), 6.69 (d, J = 8.5 Hz, 1H), 6.37 (d, J = 16.0 Hz, 1H), 4.94 (br), 4.21 (q, J = 7.0 Hz, 2H), 1.31 (t, J = 7.0 Hz, 3H). ^{13}C NMR (125 MHz, CD_3OD): 169.6, 159.2, 147.9, 146.6, 145.7, 144.3, 132.4, 126.1, 123.3, 119.6, 118.7, 116.7, 115.6, 113.3, 111.7, 99.2, 61.5, 14.6. ESMS m/z: 339.4 $(M - 1)^-$.

*4.1.4.12. (E)-Ethyl 3-(2-(3,4-dihydroxyphenyl)-7-hydroxybenzofuran-5-yl)acrylate (**5m**).* Yield: 57%. Mp = 183–186 °C. IR νmax: 3342, 1686, 1629, 1282 cm^{-1}. ^1H NMR (600 MHz, CD_3OD): 7.67 (d, J = 15.5 Hz, 1H), 7.32 (d, J = 2.0 Hz, 1H), 7.26 (dd, J = 8.5, 2.0 Hz, 1H), 7.25 (br), 6.96 (d, J = 2.0 Hz, 1H), 6.89 (s, 1H), 6.85 (d, J = 8.5 Hz, 1H), 6.38 (d, J = 15.5 Hz, 1H), 4.23 (q, J = 7.2 Hz, 2H), 1.31 (t, J = 7.2 Hz, 3H). ^{13}C NMR (150 MHz, CD_3OD): 169.2, 158.8, 147.7, 147.3, 146.6, 146.0, 143.7, 133.2, 131.7, 123.5, 118.4, 117.1, 116.8, 114.4, 113.2, 110.0, 100.6, 61.7, 14.6. ESMS m/z: 339.2 $(M - 1)^-$.

*4.1.4.13. (E)-Ethyl 3-(7-hydroxy-2-(3,4,5-trihydroxyphenyl)benzofuran-5-yl)acrylate (**5n**).* Yield: 64%. Mp = 234–239 °C. IR νmax: 3412, 1685, 1629, 1451, 1287 cm^{-1}. ^1H NMR (600 MHz, CD_3OD): 7.67 (d, J = 16.2 Hz, 1H), 7.25 (d, J = 1.2 Hz, 1H), 6.94 (d, J = 1.2 Hz,1H), 6.91 (s, 2H), 6.85 (s, 1H), 6.39 (d, J = 16.2 Hz, 1H), 4.23 (q, J = 7.2 Hz, 2H), 1.32 (t, J = 7.2 Hz, 3H). ^{13}C NMR (150 MHz, CD_3OD): 169.1, 159.1, 147.3, 147.2, 146.1, 143.8, 135.8, 133.2, 131.7, 122.5, 117.1, 114.3, 109.9, 105.5, 100.7, 61.6, 14.6. ESMS m/z: 355.2 $(M - 1)^-$.

*4.1.4.14. (E)-Ethyl 3-(4,5-dihydroxy-2-(7-hydroxybenzofuran-2-yl) phenyl)acrylate (**5o**).* Yield: 62%. Mp = 171–176 °C. IR νmax: 3256, 2925, 1685, 1368, 1297 cm^{-1}. ^1H NMR (400 MHz, CD_3OD): 8.09 (d, J = 16.0, 1H), 7.25 (s, 1H), 7.18 (s, 1H), 7.08 (t, J = 8.0 Hz, 1H), 7.06 (dd, J = 8.0, 1.0 Hz, 1H), 6.74 (dd, J = 8.0, 1.0 Hz, 1H), 6.66 (s, 1H), 6.30 (d, J = 16.0 Hz, 1H), 4.22 (q, J = 7.0 Hz, 2H), 1.30 (t, J = 7.0 Hz, 3H). ^{13}C NMR (125 MHz, CD_3OD): 169.2, 155.3, 149.1, 147.8, 145.0, 144.7, 143.6, 132.3, 126.1, 125.3, 124.8, 117.8, 116.5, 114.4, 113.0, 111.7, 107.5, 61.6, 14.6. ESMS m/z: 339.1 $(M - 1)^-$.

*4.1.4.15. 5-Bromo-2-(4-hydroxyphenyl)benzofuran-7-ol (**5p**).* Yield: 52%. Mp = 255–258 °C. IR νmax: 3358, 1584, 1469, 1209 cm^{-1}. ^1H NMR (600 MHz, CD_3OD): 7.73 (dd, J = 6.6, 1.8 Hz, 2H), 7.14 (d, J = 1.8 Hz, 1H), 6.86 (d, J = 6.6 Hz, 2H), 6.85 (d, J = 1.8 Hz, 1H), 6.80 (d, J = 1.8 Hz, 1H). ^{13}C NMR (150 MHz, CD_3OD): 159.7, 158.9, 144.3, 146.6, 134.2, 127.7, 122.9, 116.7, 116.6, 115.2, 114.1, 99.9. ESMS m/z: 305.1 $(M - 1)^-$.

*4.1.5. General procedure for the synthesis of (E)-Ethyl 3-(4,5-dimethoxy-2-(7-methoxybenzofuran-2-yl)phenyl)acrylate (**9a**)*

To a dry pressure tube was added **4a** (180 mg, 0.50 mmol), $Pd(OAc)_2$ (5 mg, 0.02 mmol), triphenylphosphine (16 mg, 0.06 mmol) and Et_3N (0.14 mL, 0.99 mmol) in degassed DMF (15 mL) under nitrogen was added ethyl acrylate (0.081 mL, 0.74 mmol). Ethyl acrylate was degassed before being added to the reaction mixture. The tube was then sealed and the mixture was heated to 110 °C with stirring for 24 h. The reaction was cooled to ambient temperature and the solvent was removed under high vacuum. The residue was purified by column chromatography to yield **9a** (136 mg, 71%) as a white solid. IR νmax: 3448, 2929, 1716, 1519, 1274, 1205 cm^{-1}. ^1H NMR (500 MHz, $CDCl_3$): 8.12 (d, J = 15.6 Hz, 1H), 7.32 (s, 1H), 7.19 (d, J = 8.0 Hz, 1H), 7.16 (t, J = 8.0 Hz, 1H), 7.10 (s, 1H), 6.82 (d, J = 8.0 Hz, 1H), 6.71 (s, 1H), 6.34 (d, J = 15.5 Hz, 1H), 4.24 (q, J = 7.0 Hz, 2H), 4.03 (s, 3H), 3.97 (s, 3H), 3.94 (s, 3H), 1.31 (t, J = 7.0 Hz, 3H). ^{13}C NMR (125 MHz, $CDCl_3$): 167.0, 153.4, 150.5, 149.5, 145.3, 144.1, 142.9, 130.8, 126.0, 124.4, 123.7, 118.5, 113.5, 111.1, 109.3, 107.5, 106.9, 60.4, 56.2, 56.1, 56.0, 14.3. ESMS m/z: 787.2 $(2M + 23)^+$.

4.2. Inhibition assay for α-glucosidase activity

All synthetic compounds were evaluated for α-glucosidase inhibition activity. We purchased α-glucosidase (isolated from *S. cerevisiae*) and 4-nitrophenyl α-D-glucopyranoside (4-NPGP) from Sigma Chemical Co. (St. Louis, MO, USA). Inhibitory activity was measured according to Chu, Wu and Hsieh (2014). Briefly, the quantity of 4-nitrophenol released from 4-NPGP was measured using a UV–Vis spectrophotometer at 405 nm. The reaction mixture, comprising 20 μL of the test compound at various concentrations (0–100 μM), was premixed with 120 μL of 100 mM phosphate buffer solution (pH 7.0). Following incubation at 30 °C for 10 min, 40 μL of 12.5 mM 4-NPGP was added, and the absorbance at 405 nm was measured using a VersaMax microplate reader (Molecular Devices Corporation, Sunnyvale, CA, USA). Resveratrol and quercetin were used as positive controls in this α-glucosidase inhibition assay. IC_{50} values were defined as the concentration of compound required to inhibit 50% of α-glucosidase activity under assay conditions.

4.3. DPPH radical scavenging assays

The free radical scavenging activity of each hydroxyl-functionalized 2-arylbenzo[*b*]furan was evaluated using 1,1-diphenyl-2-picrylhydrazyl (DPPH) free radicals. The reactions were performed in 96-well microplates with each well containing 150 μL of the final reaction mixture. The test compound was dissolved in MeOH at varying concentrations (0–100 μM) and mixed with 0.1 mM DPPH at 37 °C for 5 min. The absorbance was read using a microplate spectrophotometer at 517 nm. Antioxidant activity was determined according to the IC_{50} value of DPPH.

4.4. Kinetics involved in the inhibition of α-glucosidase

Lineweaver–Burk plot analysis was performed to determine the inhibition mode of hydroxyl-functionalized 2-arylbenzo[*b*]furans **5a** and **5n**, and kinetics were measured using increasing concentrations of 4-NPGP as a substrate in the absence or presence of various concentrations of hydroxyl-functionalized 2-arylbenzo[*b*]furans **5a** and **5n**. Dixon plot analysis was used to determine the competitive inhibition constant (*Ki*) and uncompetitive inhibition constant (*Ki′*). *Ki* expresses the equilibrium constant for the binding of hydroxyl-functionalized 2-arylbenzo[*b*]furans **5a** and **5n** to α-glucosidase, and *Ki′* is the equilibrium constant of hydroxyl-functionalized 2-arylbenzo[*b*]furans **5a** and **5n** binding to α-glucosidase-4-NPGP complex. This study of kinetics was conducted using various concentrations of hydroxyl-functionalized 2-arylbenzo[*b*]furans, **5a** and **5n**, and 4-NPGP. The initial velocity was expressed as the absorbance rate/min at 405 nm.

4.5. Docking experiments

The 3D-structural model of the *S. cerevisiae* α-glucosidase (protein sequence entry: NP_011803, PDB code: 3A4A) was used in docking experiments. The models of compounds **5a** and **5n** were docked into the active site of the α-glucosidase based on the binding mode of maltose in *S. cerevisiae* α-glucosidase. On the basis of the structures of α-glucosidase, compounds **5a** and **5n** were manually docked into the active site with the program Coot to generate an initial binding pose of compounds **5a** and **5n** in *S. cerevisiae* α-glucosidase, respectively. These models of *S. cerevisiae* α-glucosidase-**5a** complex and *S. cerevisiae* α-glucosidase-**5n** complex were optimized by energy minimization with the program Discovery Studio, and the resulting models with most low potential energy were selected. The structure figures were generated with the program PyMOL (Schrödinger, New York, NY).

Acknowledgements

This study was supported by the National Science Council (Grant NSC 102-2113-M-077-002-MY2).

Appendix A. Supplementary data

Supplementary data related to this article can be found at http://dx.doi.org/10.1016/j.ejmech.2015.02.024.

References

[1] H. Fernemark, C. Jaredsson, B. Bunjaku, U. Rosenqvist, F.H. Nystrom, H. Guldbrand, A randomized cross-over trial of the postprandial effects of three different diets in patients with type 2 diabetes, PLoS One 8 (2013) e79324.
[2] S. Kumar, S. Narwal, V. Kumar, O. Prakash, α-Glucosidase inhibitors from plants: a natural approach to treat diabetes, Pharmacogn. Rev. 9 (2011) 19–29.
[3] F.V. Fonseca, J.R. Silva, R.I. Samuels, R.A. DaMatta, W.R. Terra, C.P. Silva, Purification and partial characterization of a midgut membrane-bound α- glucosidase from Quesada gigas (Hemiptera: Cicadidae), Comp. Biochem. Physiol. B 155 (2010) 20–25.
[4] T. Hara, J. Nakamura, N. Koh, F. Sakakibara, N. Takeuchi, N. Hotta, An importance of carbohydrate ingestion for the expression of the effect of alpha-glucosidase inhibitor in NIDDM, Diabetes Care 19 (1996) 642–647.
[5] S. Ogawa, M. Kanto, Design and synthesis of 5a-carbaglycopyranosylamime glycosidase inhibitors, Curr. Top. Med. Chem. 9 (2009) 58–75.
[6] G. Derosa, P. Maffioli, α-Glucosidase inhibitors and their use in clinical practice, Arch. Med. Sci. 9 (2012) 899–906.
[7] S. Yamagishi, T. Matsui, S. Ueda, K. Fukami, S. Okuda, Clinical utility of acarbose, an alpha-glucosidase inhibitor in cardiometabolic disorders, Curr. Drug Metab. 10 (2009) 159–163.
[8] P.B. Fischer, M. Collin, G.B. Karlsson, W. James, T.D. Butters, S.J. Davis, S. Gordon, R.A. Dwek, F.M. Platt, The alpha-glucosidase inhibitor *N*-butyl-deoxynojirimycin inhibits human immunodeficiency virus entry at the level of post-CD4 binding, J. Viol. 69 (1995) 5791–5797.
[9] S. Atsumi, C. Nosaka, Y. Ochi, H. Iinuma, K. Umezawa, Inhibition of experimental metastasis by an alpha-glucosidase inhibitor, 1,6-epi-cyclophellitol, Cancer Res. 53 (1993) 4896–4899.
[10] J.P. Chambers, A.D. Elbein, J.C. Williams, Nojirimycin-a potent inhibitor of purified lysosomal alpha-glucosidase from human liver, Biochem. Biophys. Res. Commun. 107 (1982) 1490–1496.
[11] R. Saul, J.J. Ghidoni, R.J. Molyneux, A.D. Elbein, Castanospermine inhibits alpha-glucosidase activities and alters glycogen distribution in animals, Proc. Natl. Acad. Sci. U. S. A. 82 (1985) 93–97.
[12] A.D. Rodríguez-Carrizalez, J.A. Castellanos-González, E.C. Martínez-Romero, G. Miller-Arrevillaga, D. Villa-Hernández, P.P. Hernández-Godínez, G.G. Ortiz, F.P. Pacheco-Moisés, E.G. Cardona-Muñoz, A.G. Miranda-Díaz, Oxidants, antioxidants and mitochondrial function in non-proliferative diabetic retinopathy, J. Diabetes 6 (2014) 167–175.
[13] R. Gupta, M. Mathur, V.K. Bajaj, P. Katariya, S. Yadav, R. Kamal, R.S. Gupta, Evaluation of antidiabetic and antioxidant activity of Moringa oleifera in experimental diabetes, J. Diabetes 4 (2012) 164–171.
[14] E. Ladopoulou, A.N. Matralis, A.P. Kourounakis, New multifunctional di-*tert*-butylphenoloctahydro(pyrido/benz)oxazine derivatives with antioxidant, antihyperlipidemic, and antidiabetic action, J. Med. Chem. 56 (2013) 3330–3338.
[15] J.V. Higdon, B. Frei, Tea catechins and polyphenols: health effects, metabolism, and antioxidant functions, Crit. Rev. Food Sci. Nutr. 43 (2003) 89–143.
[16] W. Zhou, G. Kallifatidis, B. Baumann, V. Rausch, J. Mattern, J. Gladkich, N. Giese, G. Moldenhauer, T. Wirth, M.W. Büchler, A.V. Salnikov, I. Herr, Dietary polyphenol quercetin targets pancreatic cancer stem cells, Int. J. Oncol. 37 (2010) 551–561.
[17] J. Dai, R.J. Mumper, Plant phenolics: extraction, analysis and their antioxidant and anticancer properties, Molecules 15 (2010) 7313–7352.
[18] M. Moalin, G.P. Strijdonck, M. Beckers, G. Hagemen, P. Borm, A. Bast, G.R. Haenen, A planar conformation and the hydroxyl groups in the B and C rings play a pivotal role in the antioxidant capacity of quercetin and quercetin derivatives, Molecules 16 (2011) 9636–9650.
[19] X. Liu, L. Zhu, J. Tan, X. Zhou, L. Xiao, X. Yang, B. Wang, Glucosidase inhibitory activity and antioxidant activity of flavonoid compound and triterpenoid compound from Agrimonia Pilosa Ledeb, BMC Complementary Altern. Med. 14 (2014) 12.
[20] W. Hakamata, I. Nakanishi, Y. Masuda, T. Shimizu, H. Higuchi, Y. Nakamura, S. Saito, S. Urano, T. Oku, T. Ozawa, N. Ikota, N. Miyata, H. Okuda, K. Fukuhara, Planar catechin analogues with alkyl side chains: a potent antioxidant and an alpha-glucosidase inhibitor, J. Am. Chem. Soc. 128 (2006) 6524–6525.
[21] Y.L. Lin, Y.Y. Chang, Y.H. Kuo, M.S. Shiao, Anti-lipid-peroxidative principles from Tournefortia sarmentosa, J. Nat. Prod. 65 (2002) 745–747.
[22] Z. Fang, Y. Song, T. Sarkar, E. Hamel, W.E. Fogler, G.E. Agoston, P.E. Fanwick, M. Cushman, Stereoselective synthesis of 3,3-diarylacrylonitriles as tubulin polymerization inhibitors, J. Org. Chem. 73 (2008) 4241–4244.
[23] N.G. Kundu, M. Pal, J.S. Mahanty, M. De, Palladium-catalysed heteroannulation with acetylenic compounds: synthesis of benzofurans, J. Chem. Soc. Perkin Trans. 1 (1997) 2815–2820.
[24] Y.-H. Chu, S.-H. Wu, J.-F. Hsieh, Isolation and characterization of α-glucosidase inhibitory constituents from *Rhodiola crenulata*, Food Res. Int. 57 (2014) 8–14.
[25] D.P. Flaherty, T. Kiyota, Y. Dong, T. Ikezu, J.L. Vennerstrom, Phenolic bis-styrylbenzenes as β-amyloid binding ligands and free radical scavengers J, Med. Chem. 53 (2010) 7992–7999.
[26] K. Yamamoto, H. Miyake, M. Kusunoki, S. Osaki, Crystal structures of isomaltase from Saccharomyces cerevisiae and in complex with its competitive inhibitor maltose, FEBS J. 277 (2010) 4205–4214.